Vol. 20, No. 2 (2021) 541-553
Revista Mexicana de Ingeniería Química

Analysis of the transient inhibited steady-state in anaerobic digestion of a semisolid from pretreated bovine slaughterhouse wastewater

Análisis del estado estacionario inhibido transitorio en la digestión anaerobia del semisólido obtenido en el pretratamiento de aguas residuales de rastro bovino

V.C. Hernández-Fydrych[1]*, G. Benítez-Olivares[2], M.C. Fajardo-Ortiz[1], U. Rojas-Zamora[2], M.L. Salazar-Peláez[3]*

[1]*Departamento de Biotecnología. División de Ciencias Biológicas y de la Salud. Universidad Autónoma Metropolitana-Iztapalapa, Av. San Rafael Atlixco 186, Col. Vicentina, 09340, Ciudad de México, México.*
[2]*Departamento de Ingeniería de Procesos e Hidráulica. División de Ciencias Básicas e Ingeniería, Universidad Autónoma Metropolitana-Iztapalapa, Av. San Rafael Atlixco 186, Col. Vicentina, 09340, Ciudad de México, México.*
[3]*Departamento de Ciencias Básicas. División de Ciencias Básicas e Ingeniería, Universidad Autónoma Metropolitana-Azcapotzalco, Av. San Pablo 180, Col. Reynosa Tamaulipas, 02200, Ciudad de México, México.*

Received: September 4, 2020; Accepted: December 16, 2020

Abstract

This work aimed to analyze the methane production dynamics and the conditions leading to a transient-inhibited steady-state phase in anaerobic digestion of physically pretreated slaughterhouse wastewater. The mathematical analysis provided complementary information for applications at the real scale. The pretreatments consisted of autoclaving (120 °C, 1.2 atm, 60 min), which generated the semisolid, and homogenization (30000 rpm, 1 minute). The semisolid was the substrate for a biochemical methane production test, carried out at room temperature with a volumetric substrate to inoculum (S/I) ratio of 3:1. The methane production kinetics were complex and followed a stepped curve with four stages: 1) exponential phase, 2) transient partial methanogenesis inhibition, 3) recovery phase and 4) substrate depletion phase. FTIR analysis showed that semisolid had high contents of aliphatic and nitrogen compounds, while anaerobic digestion led to reductions of amines I and II, other amides, and aliphatic structures and the production of several amino acids. Mathematical models employed to predict cumulative methane production (Gompertz, Richards, Luedeking-Piret, and Modified first-rate) showed a good fit and low percentage error, although none of them accurately forecasted the transient inhibited steady-state (2nd phase).

Keywords: acetic acid, ammonium, BMP tests, inhibited steady-state, methane kinetics.

Resumen

En este trabajo se analizó la producción de metano y las condiciones que condujeron a un estado estacionario inhibido transitorio en la digestión anaerobia de aguas residuales de rastro pretratadas. Se utilizó un pretratamiento térmico en autoclave (120 ºC, 1,2 atm, 60 min) que generó el semisólido, y homogeneización (30000 rpm, 1 minuto). Este semisólido fue el sustrato para las pruebas de potencial bioquímico de metano, llevadas a cabo a temperatura ambiente con una relación sustrato a inóculo de 3:1. La cinética de producción de metano fue compleja y siguió una curva escalonada con cuatro etapas: 1) fase exponencial, 2) fase de inhibición parcial de la metanogénesis, 3) fase de recuperación y 4) fase de agotamiento del sustrato. El análisis FTIR mostró que el semisólido tenía alto contenido de compuestos alifáticos y nitrogenados, mientras que la digestión anaerobia redujo las aminas I y II, amidas y otras estructuras alifáticas y produjo varios aminoácidos. Los modelos matemáticos empleados para predecir la producción acumulada de metano (Gompertz, Richards, Luedeking-Piret y Primer orden modificado) mostraron un buen ajuste y bajo porcentaje de error, aunque ninguno de ellos pronosticó con precisión el estado estacionario inhibido transitorio (segunda fase).

Palabras clave: ácido acético, amonio, pruebas PBM, estado estacionario inhibido, cinética de metano.

* *Corresponding author. E-mail*: monsalazar@azc.uam.mx
Tel. 52-55-53-18-93-60
https://doi.org/10.24275/rmiq/IA2012
ISSN:1665-2738, *issn-e*: 2395-8472

1 Introduction

Slaughterhouse wastewater (SWW) is a residue characterized by a high load of animal derivatives, such as blood and inedible tissues, and pathogenic organisms, making it a potential risk to animal and human health (Franke-Whittle and Insam, 2013; Cárdenas-Medina *et al*., 2020). Additionally, the large volumes of SWW produced become its management a challenge, as its improper and unsafe disposal can cause serious environmental issues (Arvanitoyannis and Ladas, 2008).

SWW treatment involves several processes, including anaerobic digestion (AD), composting, alkaline hydrolysis, and incineration (Harris and McCabe, 2015). Among these treatments, AD stands out as it has the additional advantages of nutrient recycling and methane production (Franke-Whittle and Insam, 2013; Cárdenas-Medina *et al*., 2020). Indeed, SWW is considered a suitable substrate for AD due to its high methane yield potential (Palatsi *et al*., 2011); however, the high protein concentration usually found in SWW can lead to AD inhibition as a consequence of ammonium (NH_4^+) and long-chain fatty acid (LCFA) accumulation, which are by-products of protein and fat hydrolysis (Hernández-Fydrych *et al*., 2018). Moreover, biomass can absorb lipids and form floating aggregates and foam, leading to stratification and causing operating problems in wastewater treatment plants (Cuetos *et al*., 2010a). Pretreatment of SWW helps overcome these problems by enhancing the hydrolysis rate, which is considered the limiting step of the AD process. Thus, substrate availability and removal can be improved, increasing the reaction kinetics and biogas production (Harris and McCabe, 2015).

Several pretreatments, including physical, chemical, and biological processes, have been tested for SWW components' hydrolysis. Among these, thermal pretreatments are highly efficient as they allow the release and solubilization of complex organics compounds, compensating for the energy demand by the considerable increase in the biogas production rate (Carrère *et al*., 2010). In turn, mechanical pretreatments can accelerate the anaerobic digestion of SWW by increasing the surface area to volume ratio and homogenization of the feed (Izumi *et al*., 2010).

Moreover, AD of SWW leads to complex kinetics, which is not fully understood and has an elongated S-shape or a stepped curve (Wang *et al*., 2015) due to several substrates' presence, such as fats, and proteins, with different hydrolysis rates (Ware and Power, 2017). Therefore, it is necessary to evaluate the anaerobic degradation dynamics of SWW through analysis of experimental results and mathematical models. In general, these models fit methane production adequately with simple substrates (APHA-AWWA-WEF, 2018), but they cannot describe the kinetics of complex substrates with an inhibited steady-state phase.

A previous investigation (Hernández-Fydrych *et al*., 2019) found that thermal pretreatment of SWW produces a semisolid, which has a high methane yield as it concentrates most of the organic matter in SWW in a small volume; however, doubts regarding the anaerobic digestion of SWW remain, including the processes that lead to complex kinetics for methane production as well as the generation of inhibitory substances.

Thus, this work aimed to analyze the dynamics of methane production and the conditions leading to an inhibited steady-state phase in the anaerobic digestion of the semisolid obtained after thermal pretreatment of SWW. Furthermore, the mathematical analysis provides complementary information for applications on a real scale.

2 Materials and methods

2.1 SWW sampling and characterization

SWW sampling was performed in a municipal slaughterhouse with a capacity of 80 bovines per day. Samples were meshed in situ through a 5 mm screen and stored at 4 °C. The content of the organic matter (measured as COD_S), nitrogen (measured as NH_4^+-N), and solids (measured as TS, VS, FS) were determined according to the Standard Methods (APHA-AWWA-WEF, 2018). The soluble protein concentration was analyzed through the Lowry method (Lowry *et al*., 1951), while a benchtop pH meter (Orion StarTM A211, Thermo Fischer Scientific, USA) served to determine pH.

2.2 SWW physical pretreatments

First, the thermal pretreatment was autoclaving (Model CV 300, AESA, Mexico) at 120 °C and 1.2 atm for one hour, leading to the appearance of a liquid and a semisolid phase, which deposited. A fraction

of the semisolid was also subjected to a mechanical pretreatment, consisting of homogenization (Tissue Tearer, Model 985-370, Biospec Products Inc., USA) for one minute at 30000 rpm (Hernández-Fydrych *et al*., 2019). Thus, the substrates for BMP tests were the semisolid obtained after SWW thermal treatment (S) and the semisolid that also underwent mechanical treatment (SM).

2.3 Biomethane potential (BMP) test

Anaerobic granular sludge from a cannery wastewater treatment plant, with a 52.12 g VS/L content, served as inoculum in the BMP test. The sludge was washed with phosphate buffer and stored at 4°C before starting the test.

Hernández-Fydrych *et al*., (2019) analyzed the influence of the volumetric ratio in methane production using S and SM as substrate and found the highest methane production rate at 3:1 substrate/inoculum ratio; therefore, this ratio was used in the test, and it was equivalent to 12.5 mL inoculum and 37.5 mL of semisolid. Thereby, thirty-six serological bottles (18 for S and 18 for SM) were incubated at room temperature for 135 days and, approximately every two weeks, three of these bottles were opened to determine the contents of COD_S, NH_4^+-N, and solids according to the methods described in section 2.1.

Also, the volatile fatty acid (VFA) concentration and composition were analyzed by gas chromatography (GC-FID) (Clarus 580, PerkinElmer), using a capillary AT-1000 column (Alltech) with nitrogen as the carrier gas.

Biogas production was quantified daily by saline solution displacement, and its composition was determined twice a week by gas chromatography (TCD-GC) in a Carbosphere 80/100 stainless steel packed column (Alltech) with helium as the carrier gas (Gow-Mac Series 580, Gow-Mac Instrument Co, Bethlehem, PA, USA). The specific methane yield (SMY), expressed as L CH_4/g VS, is the total volume of methane produced during the test period per initial substrate concentration, and it was the parameter employed to evaluate the substrates' methane potential. These calculations were performed under normal conditions (20 °C, 1 atm).

2.4 Fourier transform infrared spectroscopy (FTIR) analysis

Samples of SWW, both semisolids (S and SM), and the digestates obtained during the BMP test were freeze-dried for 24 hours (VirTis BenchTop 2K, SP Industries Inc., USA). Triplicate samples were analyzed by infrared (IR) using an FTIR spectrometer (ALPHA II, Bruker, Germany) in the absorbance range of 4000-400 cm^{-1} at a rate of 0.5 $cm{\cdot}s^{-1}$.

2.5 Models used to predict methane production of pretreated SWW

Four mathematical models fitted the experimental data in this work (Table 1).

Table 1. Models used to predict methane production from SWW.

Modified Gompertz (Zwietering *et al*., 1990)	$P_G(t) = \epsilon_{Pe}\left[-e^{\frac{\mu_{max,Pe(1)}}{\epsilon_P}(\lambda_P - t)} + 1\right]$
Richards (Ware and Power 2017)	$P_R(t) = \epsilon_P\left[1 + \kappa_P e^{(1+\kappa_P)} e\left[\frac{\mu_{max,P}}{\epsilon_P}(1+\kappa_P)\left(1+\frac{1}{\kappa_P}\right)(\lambda_P - t)\right]\right]^{\frac{1}{\kappa_P}}$
Logistic (Fujikawa *et al*., 2004)	$X(t) = \frac{X_{max}}{1 + \left[\left(\frac{X_{max}-X_0}{X_0}\right)e^{-\mu_{max}t}\right]}$
Luedeking-Piret (Zwietering *et al*., 1990)	$P(X) = P_0 + \alpha_P(X - X_0) - \beta_P \frac{X_{max}}{\mu_{max}} \ln\left(\frac{X_{max} - X_0}{X_{max} - X}\right)$
Modified first order equation (Wellinger *et al*., 2013)	$P_w(t) = P_{wmax}\left(1 - \gamma P e^{-k_1 t} - (1 - \gamma P)e^{-k_2 t}\right)$

These predictive models served to describe the methane production observed during the BMP test. The modified Gompertz equation (Zwietering *et al.*, 1990) is an empirical nonlinear regression model commonly employed to simulate methane production (Kafle and Chen, 2016).

Where: $P_G(t)$ is the methane produced over time, ϵ_p is the maximum specific methane production potential, μ_{max}, P is the maximum specific methane production rate, and λ_P is the lag phase.

Richard's sigmoidal model is a modification of the logistics model focused on methane production and provides flexibility in the curve by incorporating a fourth parameter (κ_P). This parameter is between the minimum and maximum asymptote (Ware and Power, 2017); thus, PR(t) is methane production as a function of time.

The logistic model forecasts the cell growth rate and biomass concentration, which serve to predict methane production in the Luedeking-Piret model (Fujikawa *et al.*, 2004; Zwietering *et al.*, 1990).

In the logistic model, $X(t)$ is the biomass concentration over time, X_{max} is the maximum concentration of biomass, and μ_{max} is the maximum specific growth rate. In the Luedeking-Piret model, $P(x)$ is the methane production rate as a function of biomass growth, P_0 is the initial value of methane production, and α_p and β_p are coefficients associated with the yields of biomass and methane, respectively. The modified first-order equation associates methane production with the biodegradability of simple and complex substrates (Yang *et al.*, 2015). Thus, $P_w(t)$ is methane production, P_{wmax} is the maximum methane cumulative yield, and λ_p is the proportion of easily degradable substrates, while k_1 and k_2 are the first-order rate constants for the readily and hardly degradable substrates, respectively.

A nonlinear least-squares regression analysis, using a 64-bit version of Matlab software R2017b (9.3.0.713579), was performed on these models. Minimizing the sum of the squares of the differences between the predicted and measured values allowed the equation coefficients (ϵ_p, μ_{max}, P, κ_P, X_{max}, μ_{max}, P_0, α_p, β_p, P_{wmax}, k_1, and k_2) to be determined (Benítez-Olivares *et al.*, 2016). The regression data analysis tool was used to calculate the correlation coefficient (R^2), while the comparison between the predicted and measured specific methane yields fitted the minimized percentage error. These parameters served to determine the model that better forecasts methane production in the BMP test.

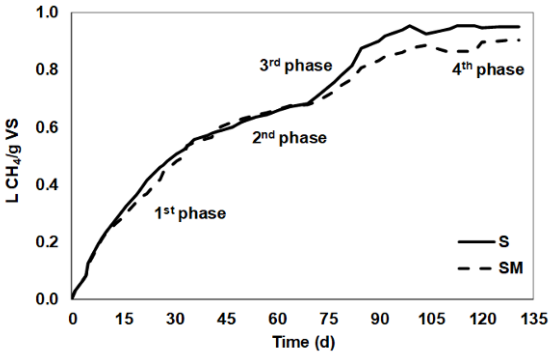

Fig. 1. Cumulative methane production for the semisolid (S) and the semisolid with mechanical pretreatment (SM).

3 Results and discussion

3.1 Cumulative methane production

The cumulative methane production determined by the BMP test (Figure 1) for S and SM showed complex kinetics that followed a stepped curve, with four stages:

- 1st phase: from day 0 to 36, with a specific methane production rate (SMPR) of 0.016 LCH_4/g VS.d for S and 0.015 LCH_4/g VS.d for SM (exponential phase).
- 2nd phase: from day 36 to 69, in which the SMPR exhibited a considerable decrease to 0.004 L CH_4/ g VS.d for both substrates (S and SM).
- 3rd phase: from day 69 to 99, SMPR increased to 0.009 LCH_4/ g VS.d for S and 0.007 L CH_4/ g VS.d for SM.
- 4th phase: the last phase, in which substrate depleted and the methane production rate reached zero on day 105 (asymptotic phase)

The AD kinetics and, consequently, cumulative methane production depend on substrate biodegradability and the presence of inhibitory substances or their production during the degradation process (Labatut *et al.*, 2011).

In this sense, Ware and Power (2016a, 2016b) found methane production curves similar to those produced in the present experiment when they studied

diverse slaughterhouse solid wastes. They associated this behavior with the presence of biodegradable substrates, whose fast degradation increased the hydrolysis rate, causing a rapid build-up of acids and intermediate fermentation by-products.

Methanogenic microorganisms consumed these compounds, increasing methane production during the initial stage of the BMP test (0.016 L CH_4/g VS.d for S and 0.015 L CH_4/g VS.d for SM); however, the accumulation of ammonia and VFA inhibited the methanogenic population temporarily, in a reversible phenomenon (Chen *et al.*, 2008). Afterward, the system slowly removed the remaining VFA, and the SMPR recovered until the available substrate depletion.

The affirmations above were confirmed by the organic matter behavior over time (Figure 2a), which showed a decrease in soluble COD (COD_S) until day 26 for AD of S. Soluble proteins (ProtS) concentration raised until day 43, with the simultaneous formation of NH_4^+-N during the first 26 days (Figure 2c). These results show that hydrolysis, acidogenesis, and acetogenesis processes were carried out efficiently and contributed to the high methane production rate found in the test's exponential phase.

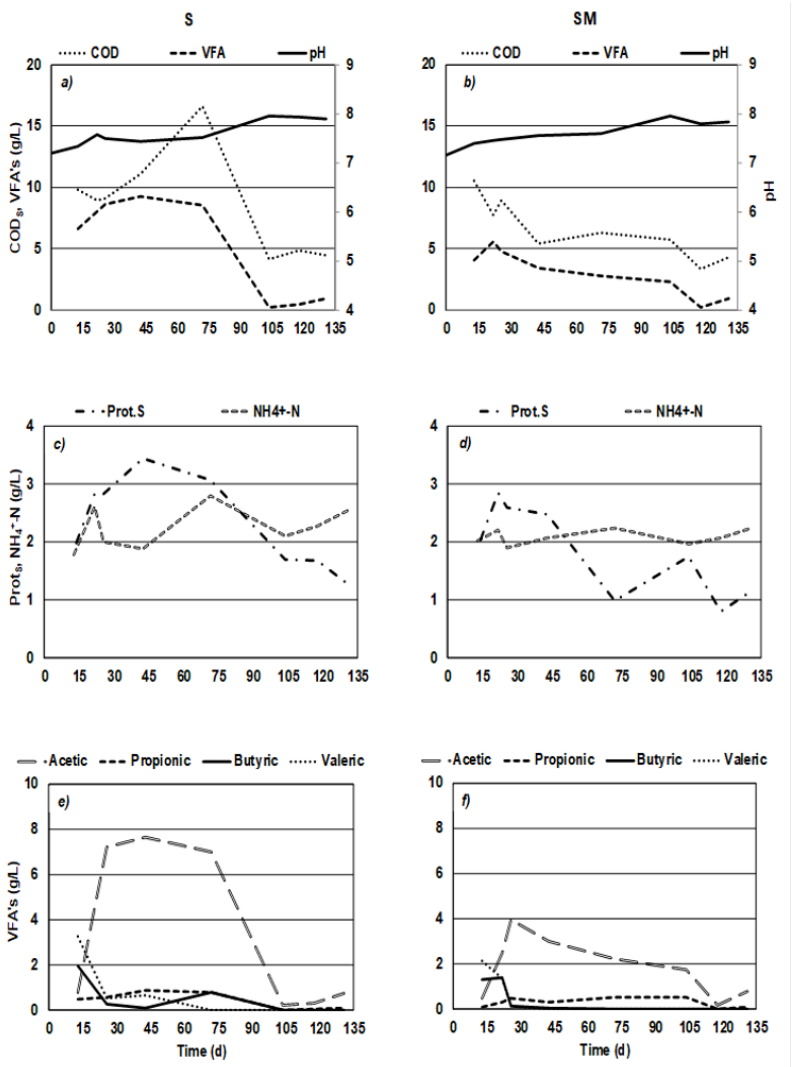

Fig. 2. Time profiles of a) and b) COD_S, VFA, and pH; c) and d) ProtS and NH_4^+-N; and e) and f) speciation of VFA for S and SM.

The organic matter (Figure 2b) and the protein (Figure 2d) profiles obtained with SM showed a decreasing trend through the test. Therefore, mechanical pretreatment helped hydrolytic enzymes to attack organic compounds in this substrate by increasing the superficial area (Izumi *et al*., 2010; Vavilin *et al*., 2008). The specific methane yield potential (SMY) of the substrates studied was 0.463 L CH_4 /g VS for S and 0.440 L CH_4 /g VS for SM. These values were similar to those in other studies with substrates such as slaughterhouse solid wastes (0.659 L CH_4 /g VS) (Ware and Power, 2016a), intestine residues (0.589 L CH_4 /g VS), and blood (0.450 L CH_4 /g VS) (Jain *et al*., 2015) and higher than the co-digestion of manure and meat-paste (0.286 L CH_4 /g VS) (Labatut *et al*., 2011). It is worth noting that these studies used incubation temperatures ranging from 35-39 °C, while in the present study, the temperature was 22 °C, which shows the high potential of the semisolid for methane production. SMY from both semisolids is related to their high content of fats and proteins (Ware and Power, 2016a), demonstrating that they are anaerobically biodegradable and have significant potential for methane production.

From days 36 to 69 (2^{nd} phase), methane production rate diminished for S and SM (0.004 L CH_4/g VS.d) due to the simultaneous accumulation of acetic acid (approximately 7.7 g/L for S and 3.0 g/L for SM) (Figures 2e and 2f) and NH_4^+-N (2.8 g/L for S and 2.2 g/L for SM) (Figures 2c and 2d). This fact led to transient methanogenesis inhibition, as acetic acid concentrations higher than 5 g/L are toxic to methanogenic organisms (Khalid *et al*., 2011). Moreover, ammonium concentrations ranging from 1.7 to 14 g/L can decrease methane concentration by 50% (Shi *et al*., 2016). Indeed, acetic acid was the predominant VFA and, together with propionic acid, was produced starting at the beginning of the test, though the former accumulated at a higher rate (Figures 2e and 2f).

This stage corresponds to an inhibited steady-state, characterized by stable but low methane production due to the acute toxic effects of both acetic acid and ammonium (Figures 2a and 2b) (Chen *et al*., 2008). In this stage, the low SMPR could be mainly associated with hydrogen-consuming methanogenic microorganisms since the acetoclastic methanogens' specific activity decreases at high concentrations of these compounds (Song *et al*., 2010). According to Zheng *et al*., (2021), in the AD of nitrogen-rich wastewaters, with lower carbon content, as SWW, ammonia tends to accumulate because it is a by-product of the AD of these substrates; also, the microorganisms do not fully utilize it in the reactor. Additionally, it is well known that ammonia is an inhibitor of AD, leading to instability and inefficiency in the process and the accumulation of VFAs. However, high concentrations of ammonia can also act as a pH buffer, resulting in a neutral pH, even when VFAs accumulate in the system. For this reason, the AD process reaches an "inhibited steady-state", where the performance of the reactor is low but stable. Therefore, this "inhibited steady-state" results from a slight inhibition by ammonium, where both the VFAs and ammonia accumulate, partially disturbing the microbial metabolism without totally collapsing the system.

Additionally, the VFA relationships, as well as the acetic acid concentrations, have a direct correlation with AD performance and therefore can be used as indicators of digester performance; several observations have demonstrated that the propionic to acetic acids ratio (P/A) of 1:4 and an acetic acid concentration of 800 mg/L are essential for predicting impending digester failure (Zhang *et al*., 2014). In this study, the P/A ratio remained below 0.5 for both semisolids; however, the acetic acid concentration reached 7.7 g/L for S and 3.0 g/L for SM. This result indicates that the low methane production rate in the 2^{nd} phase could relate to acetoclastic methanogen inhibition since acetate increased, though the P/A ratio remained low (Zhang *et al*., 2014). The relative changes in the proportion of VFA are also indicators of AD imbalance. For instance, Fang *et al*., (2019) found that the concentration of butyrate and its isoform, isobutyrate, increased drastically shortly after a perturbation, leading to inhibition. In this study, butyric and valeric acids were consumed and did not show sudden changes during the BMP test, explaining why the AD process in this experiment only suffered transient inhibition. pH remained nearly neutral throughout the experiment (Figures 2a and 2b) since the production of ammonium from the fermentation of amino acids and the carbonic acid equilibria species buffered the system, allowing it to maintain a stable pH (Gallert and Winter, 2005). Hence, this feature favored protein hydrolysis and avoided the complete inhibition of methanogenesis, despite the high concentrations of VFA found in this phase. In the third phase (days 69 to 99), the methane production rate increased again, reaching 0.009 L CH_4/g VS.d for S and 0.007 L CH_4/g VS.d for SM, which came from hydrolysis and fermentation of remnant organics, as corroborated by the decreases in

the concentrations of COD_S (Figures 2a and 2b), ProtS (Figures 2c and 2d) and acetic acid (Figures 2e and 2f), while the pH reached a value of 8 (Figures 2a, 2b).

On days 103 and 118 for S and SM, respectively, the asymptotic phase was reached, in which substrate depleted and only hardly degradable organic matter remained; hence, methane production ceased (Figure 1). The COD_S and acetic acid concentration showed a slight increase, probably because of the residual organic compounds fermentation; nonetheless, acetic acid production was insufficient to increase methane production. Figures 2e and 2f show the speciation of VFA. Acetic acid was 62% of total VFA for S and 49% for SM, followed by isovaleric and valeric acids (18% for S and 23% for SM), isobutyric and butyric acids (11% for S and 17% for SM), and propionic acid (9% for S and 11% for SM). The amino acids released during the hydrolysis of proteins and pH are crucial factors to determine the speciation of VFA (Gallert and Winter, 2005). Acetic acid is the most relevant, considering that other VFAs must be converted into acetic acid before methane production (Kong *et al*., 2018). In turn, other VFAs, such as propionate, isobutyrate, and isovalerate, directly come from the deamination of long-chain amino acids and the β-oxidation of LCFA (Gallert and Winter, 2005).

3.2 FTIR analysis

Figure 3 shows the FTIR spectra of a) raw slaughterhouse wastewater and b) the semisolid obtained after thermal pretreatment of SWW. Both spectra presented a broad absorption band at 2500-3600 cm^{-1}, associated with O-H bonds of alcohols (3640-3610 cm^{-1}, free hydroxyl) (3500-3200 cm^{-1}, H-bonded) and carboxylic acids (3300-2500 cm^{-1}), with a strong absorption between 2800 and 3300 cm^{-1}, corresponding to C-H bonds of alkenes (3100-3000 cm^{-1}) and alkanes (3000-2850 cm^{-1}) (Bruno and Svoronos, 2011). However, the bands between 3200 and 3000 cm^{-1} disappeared in the semisolid, suggesting that thermal pretreatment helped break double bonds in SWW. Two bands near 2920 cm^{-1} and 2850 cm^{-1} appeared in both wastes, with a higher absorbance in SWW: the first corresponds to C-H bonds of aliphatic methylene, while the second represents aliphatic C-H bonds (Hafidi *et al*., 2005). These bands match fats and lipids (Rodríguez-Abalde *et al*., 2013).

Moreover, the shoulder between 3400 and 3250 cm^{-1} found in both spectra matches with N-H bonds of amines I, II, and amides, and the band at 1627 cm^{-1} corresponds with N-H bonds of amines I (Bruno and Svoronos, 2011), which remained unchanged after thermal pretreatment.

The peak between 1470 and 1450 cm^{-1} represents C-H bonds in alkanes. The band around 1300-1000 cm^{-1} could be two bands superimposed: the band around 1250-1020 cm^{-1} corresponds to C-N bonds of aliphatic amines, and the band around 1320-1000 cm^{-1} represents functional groups of alcohols, carboxylic acids, and esters (Bruno and Svoronos, 2011), as well as carbohydrates and polysaccharides (Cuetos *et al*., 2010a). Finally, the band between 800 and 400 cm^{-1} could be related to N-H bonds of amines I and II (910-650 cm^{-1}) (Bruno and Svoronos, 2011). These results showed that SWW and the semisolid were very aliphatic and had a high nitrogen compound content (associated with proteins), although thermal pretreatment decreased the amounts of carboxyl groups and double bonds.

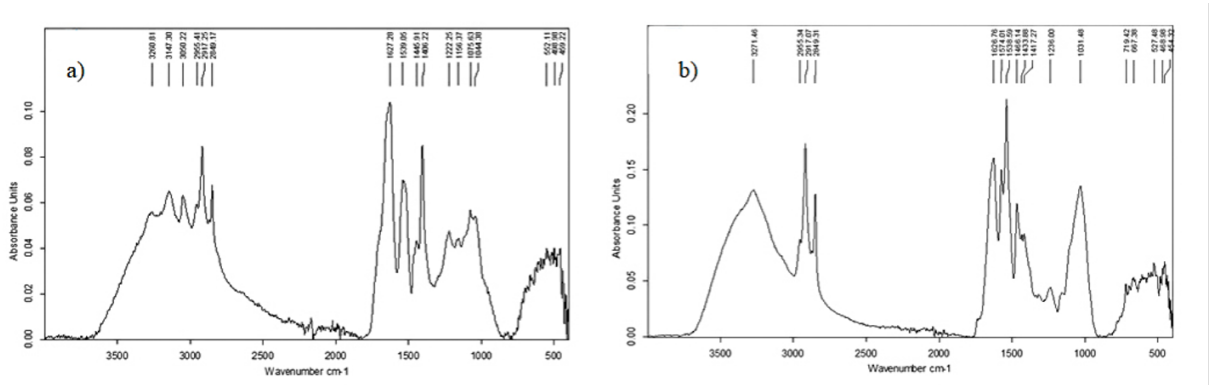

Fig. 3. FTIR spectra of a) raw slaughterhouse wastewater and b) the semisolid obtained after thermal pretreatment of SWW.

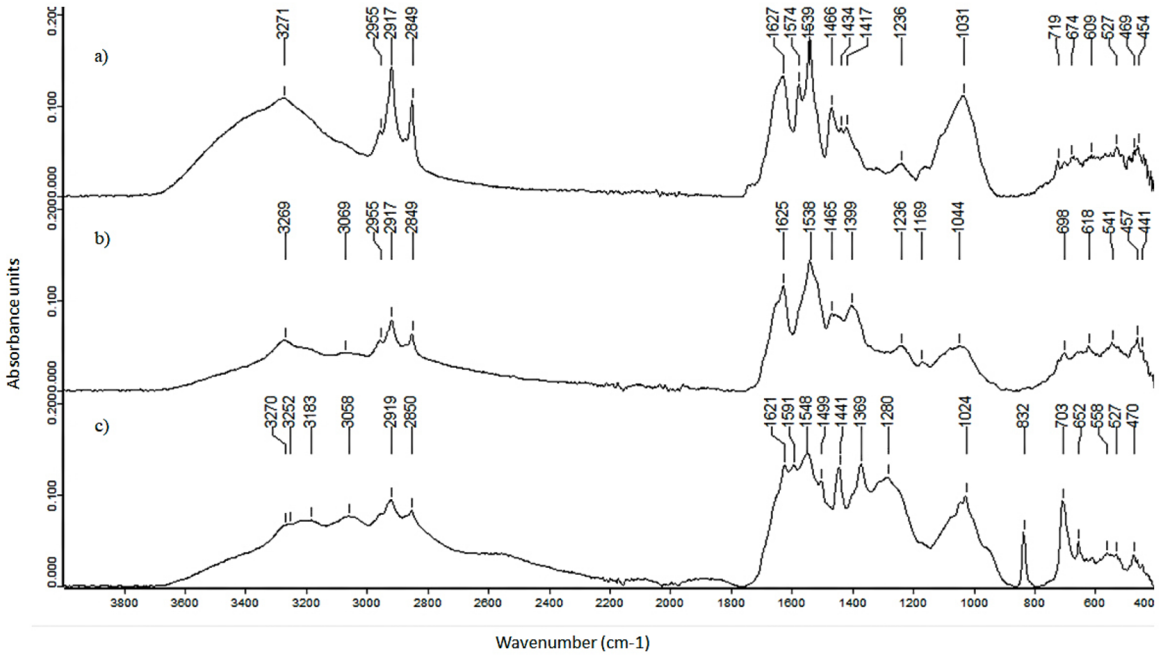

Fig. 4. Figure 4. FTIR spectra of the semisolid at different times: a) 0, b) 22 and c) 131 days.

Figure 4 shows the FTIR spectra obtained at different days (0, 22, and 131) of the BMP test. This figure reveals that the mixture of the semisolid and inoculum had a broad absorption band between 3600 and 2500 cm^{-1}, which, as mentioned before, corresponds with O-H bonds of alcohols and carboxylic acids, along with C-H bonds of alkanes.

The peak around 3270 cm^{-1}, which is related to N-H bonds of amines I, II, and amides, became sharper and practically disappeared by the end of the test. This result indicates protein hydrolysis and the reduction of aliphatic structures (Cuetos *et al*., 2010a).

Additionally, bands associated with fats and lipids (C-H stretching at 2920-2930 cm^{-1} and 2850 cm^{-1}) tended to disappear during the assay, indicating anaerobic stabilization of the semisolid and the diminution of its aliphatic structures.

The bands between 1700 and 1500 cm^{-1}, assigned to N-H bonds of amines I (1650-1580 cm^{-1}) and C=C bonds of alkenes (1680-1640 cm^{-1}), which are by-products of protein mineralization, evidence the protein hydrolysis (Cuetos *et al*., 2010b), such as amines I vibrations in the -C=O stretch of peptide bonds (1651 cm^{-1}) and amines II with an N-H bond and in the C-N stretch (1335-1250 cm^{-1}) (Kong and Yu, 2007). The bands between 2960 and 2850 cm^{-1}, which correspond to C-H bonds of aliphatic methylene in fats, decreased during the experiment and, at the same time, a new band related to the C-H bond in alkanes appeared at 1460 cm^{-1}, which is a by-product of the deformation of these structures (Rodríguez-Abalde *et al*., 2013). By the end of the BMP assay, several bands between 1700 and 1200 cm^{-1} emerged. These bands could correspond to different amino acids, such as lysine (1626-1269 cm^{-1}), asparagine (1612-1622 cm^{-1}), proline (1400-1465 cm^{-1}), glutamate (1235-1270 cm^{-1}), aspartate, and glutamic acid (both located at 1160-1253 cm^{-1}), which are produced during protein hydrolysis, as in this part of the spectra amines I and II prevail (Barth, 2007). Additionally, in this region -CH_3 (1445-1450 cm^{-1}) and -CH_2 (724-1174 cm^{-1}) bonds formed during the hydrolysis of proteins and fats (Barth, 2007). Furthermore, a peak between 1620 and 1640 cm^{-1}, characteristic of the β sheets of amines I, appeared in the three FTIR spectra (Barth, 2007; Kong and Yu, 2007). C-O bonds of alcohols, carboxylic acids, ethers, carbohydrates, and polysaccharides are in the region between 1320 and 1000 cm^{-1} (Cuetos *et al*., 2010a, 2010b). Indeed, there is evidence for the presence of carboxylic acids produced during the hydrolysis of fats and proteins, as the signals of the C=O bonds of carboxylic acids of aromatic bonds (Cuetos *et al*., 2010b) (1621 cm^{-1}) and O-H

bonds (3270 cm^{-1}) were present. Lastly, within the band around 1320-1000 cm^{-1}, which is related to the functional groups of alcohols, carboxylic acids, and esters, several peaks appeared and disappeared, showing a change in the chemical environment during the test due to anaerobic digestion.

The organic solids content in the digestate decreased by 84% by the end of the assay due to the stabilization of the organic matter in the semisolid, leaving bands between 1600 and 1000 cm^{-1}, which represent substrates available for microorganisms (Cuetos *et al*., 2009).

3.3 Model results

Figure 5 shows the fitting of the equations proposed in Section 2.4 and the experimental data in Section 3.1 (Figure 1).

This figure shows that all models overestimated methane production in the 2nd phase (inhibited steady-state). This discrepancy could have occurred because methane production decreased probably, due to the partial inhibition of acetoclastic methanogens caused by the high concentrations of ammonia and acetic acid (Figures 2c and 2d). The mathematical models, which follow sigmoidal curves, could not accurately describe this phenomenon (Harris *et al*., 2018).

Despite this result, all models had a good fit (Table 2) with the cumulative methane production found in the BMP test. The models with a lower percentage error and higher R^2 were the Richards and modified first-order rate models for both substrates. The predicted values for the specific maximum methane production (A) were very close to the experimental data (0.952 L CH_4/g VS for S and 0.904 L CH_4/g VS for SM). The Luedeking-Piret model for S (0.949 L CH_4/g VS) and the Richards model for SM (0.895 L CH_4/g VS) forecasted this parameter more accurately. These values are difficult to compare with other studies due to differences in the BMP test's environmental and operational conditions; furthermore, as far as the authors know, there are no studies in which the semisolid obtained after thermal pretreatment of slaughterhouse wastewater was the substrate in this test.

Regarding the SMPR, the values obtained with the four models were equal to those obtained analytically, and there were not significant differences between the SMPRs found for both semisolids (0.016 L CH_4/g VS.d for S and 0.015 L CH_4/g VS.d for SM). These values were similar to Ware and Power (2016a), who reported SMPRs values of 0.023 L CH_4/g VS.d with pasteurized slaughterhouse solid wastes. Hernández-Fydrych *et al*. (2019), using the same substrate, obtained an SMPR of 0.018 L CH_4/g VS.d for S and 0.014 L CH_4/g VS.d for SM. Although this parameter is proportional to the particle size (Jain *et al*., 2015), mechanical pretreatment did not affect methane production in this study, as A and SMPR were equal in both semisolids.

Thus, the substrates employed in this experiment are biodegradable and have a high methane yield potential, although their digestion period was long (131 days) due to their high concentration of pollutants (Hernández-Fydrych *et al*., 2019). This fact could favor a small volume of the digestion reactor.

The lag phase (λ) did not occur at the beginning of the BMP test. This stage indicates a delay in the hydrolysis step mainly due to the concentration of by-products that inhibit acetogenic and methanogenic bacteria (Vavilin *et al*., 2008; Ware and Power, 2016a). This result demonstrates that the pretreatment of slaughterhouse wastewater favored its degradation by accelerating the hydrolysis step.

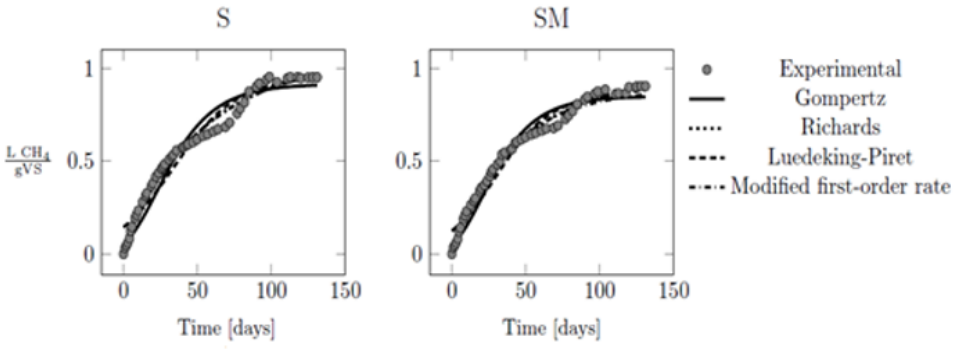

Fig. 5. Fitting of the experimental data to the Gompertz, Richards, Luedeking-Piret and modified first-rate models.

Table 2. Calculation of the relative error, R^2, SMPR and *A* for the experimental values for the different models.

Model	Error (%)		R^2		SMPR1 (L CH_4/g VS.d)		*A* (LCH_4/g VS)	
	S	SM	S	SM	S	SM	S	SM
Experimental	-	-	-	-	0.016	0.015	0.952	0.904
Gompertz	6.106	4.747	0.949	0.968	0.016	0.015	0.909	0.845
Richards	3.178	1.997	0.985	0.993	0.016	0.015	0.964	0.895
Luedeking-Piret	5.426	4.585	0.952	0.964	0.015	0.014	0.949	0.883
Modified first-order rate	3.089	2.426	0.985	0.989	0.015	0.015	0.966	0.857

[1] SMPR: specific methane production rate
[2] A: maximum methane production

Conclusions

The semisolid obtained after thermal pretreatment of slaughterhouse wastewater has a high potential for methane production (0.463 L CH_4 /g VS for S and 0.440 L CH_4 /g VS for SM) due to its high concentration of proteins and fats. Methane production from this substrate followed complex kinetics with a stepped curve and showed an inhibited steady-state caused by the accumulation of acetic acid and ammonium. FTIR analysis revealed that thermal pretreatment broke double and triple bonds in organic compounds in SWW. In contrast, during the AD process, bands corresponding to amines and fats decreased, and simultaneously, the by-products of their anaerobic degradation appeared, demonstrating organic matter mineralization. Finally, Richard's model and modified first-order rate equation showed the best fit to experimental data, although none of them adjusted the inhibited steady-state accurately.

Acknowledgements

The authors are thankful to Dr. Patricia Castilla Hernández, Dr. Yara Ramírez-Quirós, and Aldo Farías Hernández for their assistance with the experimental work. The first author expresses her gratitude to CONACyT for the scholarship granted to study her doctorate.

Nomenclature

Anaerobic digestion (AD)
Biochemical methane production (BMP)
Fixed solids (FS)
Fourier transform infrared spectroscopy (FTIR)
Gas chromatography (GC-FID)
Long-chain fatty acids (LCFA)
Propionic to the acetic acid ratio (P/A)
Semisolid (S)
Semisolid with mechanical pretreatment (SM)
Slaughterhouse wastewater (SWW)
Soluble chemical oxygen demand (COD_S)
Soluble proteins (ProtS)
Specific methane production rate (SMPR)
Specific methane yield (SMY)
Total solids (TS)
Volatile fatty acids (VFA)
Volatile solids (VS)

References

American Public Health Association, American Water Works Association, Water Environment Federation. (2018). Standard methods for the examination of water and wastewaterAmerican Public Health Association, American Water Works Association, Water Environment Federation, 2018. Standard methods for the examination of water and wastewater. American Public Health Asso. American Public Health Association.

Arvanitoyannis, I.S., Ladas, D. (2008). Meat waste treatment methods and potential uses. *International Journal of Food Science & Technology 43*, 543-559. https://doi.org/10.1111/j.1365-2621.2006.01492.x

Barth, A. (2007). Infrared spectroscopy of proteins. *Biochimica et Biophysica Acta - Bioenergetics 1767*, 1073-1101. https://doi.org/10.1016/j.bbabio.2007.06.004

Benítez-Olivares, G., Valdés-Parada, F.J., Saucedo-Castañeda, J.G. (2016). Derivation of an

upscaled model for mass transfer and reaction for non-food starch conversion to bioethanol. *International Journal of Chemical Reactor Engineering 14*, 1115-1148. https://doi.org/10.1515/ijcre-2016-0004

Bruno, T.J., Svoronos, P.D.N. (2011). *Handbook of Basic Tables for Chemical Analysis*. CRC Press.

Cárdenas-Medina, K.N., Fajardo-Ortiz, M.C., Schettino-Bermúdez, B.S., Meraz-Rodríguez, M. A. and Castilla-Hernández, P. (2020). Acidogenesis/Metanogenesis from acid cheese whey in hybrid-UASB reactors. *Revista Mexicana de Ingeniería Química 19*, 17-27. https://doi.org/10.24275/rmiq/IA1420

Carrère, H., Dumas, C., Battimelli, A., Batstone, D.J., Delgenès, J.P., Steyer, J.P., Ferrer, I. (2010). Pretreatment methods to improve sludge anaerobic degradability: A review. *Journal of Hazardous Materials 183*, 1-15. https://doi.org/10.1016/j.jhazmat.2010.06.129

Chen, Y., Cheng, J.J., Creamer, K.S. (2008). Inhibition of anaerobic digestion process: A review. *Bioresource Technology 99*, 4044-4064. https://doi.org/10.1016/j.biortech.2007.01.057

Cuetos, M.J., Gómez, X., Otero, M., Morán, A. (2010a). Anaerobic digestion and co-digestion of slaughterhouse waste (SHW): Influence of heat and pressure pre-treatment in biogas yield. *Waste Management 30*, 1780-1789. https://doi.org/10.1016/j.wasman.2010.01.034

Cuetos, M.J., Gómez, X., Otero, M., Morán, A. (2010b). Anaerobic digestion of solid slaughterhouse waste: Study of biological stabilization by Fourier Transform infrared spectroscopy and thermogravimetry combined with mass spectrometry. *Biodegradation 21*, 543-556. https://doi.org/10.1007/s10532-009-9322-7

Cuetos, M.J., Morán, A., Otero, M., Gómez, X. (2009). Anaerobic co-digestion of poultry blood with OFMSW: FTIR and TG-DTG study of process stabilization. *Environmental Technology 30*, 571-582. https://doi.org/10.1080/09593330902835730

Fang, W., Zhang, X., Zhang, P., Wan, J., Guo, H., Ghasimi, D.S.M., Morera, X.C., Zhang, T. (2019). Overview of key operation factors and strategies for improving fermentative volatile fatty acid production and product regulation from sewage sludge. *Journal of Environental Science 87*. https://doi.org/10.1016/j.jes.2019.05.027

Franke-Whittle, I.H., Insam, H. (2013). Treatment alternatives of slaughterhouse wastes, and their effect on the inactivation of different pathogens: A review. *Critical Reviews in Microbiology 39*, 139-151. https://doi.org/10.3109/1040841X.2012.694410

Fujikawa, H., Kai, A., Morozumi, S. (2004). A new logistic model for *Escherichia coli* growth at constant and dynamic temperatures. *Food Microbiology 21*, 501-509. https://doi.org/10.1016/j.fm.2004.01.007

Gallert, C., Winter, J. (2005). Bacterial metabolism in wastewater treatment systems. In: Jördering, H.J., Winter, J. (Eds.), E*nvironmental Biotechnology. Concepts and Applications*. Wiley-VCH Verlag, pp. 1-48.

Hafidi, M., Amir, S., Revel, J.-C. (2005). Structural characterization of olive mill waster-water after aerobic digestion using elemental analysis, FTIR and ^{13}C NMR. *Process Biochemistry 40*, 2615-2622. https://doi.org/10.1016/j.procbio.2004.06.062

Harris, P.W., McCabe, B.K. (2015). Review of pre-treatments used in anaerobic digestion and their potential application in high-fat cattle slaughterhouse wastewater. *Applied Energy 155*, 560-575. https://doi.org/10.1016/j.apenergy.2015.06.026

Harris, P.W., Schmidt, T., Mccabe, B.K. (2018). Journal of Environmental Chemical Engineering Bovine bile as a bio-surfactant pre-treatment option for anaerobic digestion of high-fat cattle slaughterhouse waste. *Journal of Environmental Chemical Engineering 6*, 444-450. https://doi.org/10.1016/j.jece.2017.12.034

Hernández-Fydrych, V.C., Castilla-Hernández, P., Beristain-Cardoso R., Trejo-Aguilar, G.M. and Fajardo-Ortiz, M.C. (2018). COD and

Ammonium removal in SBR operated under different combinations using pre-treated slaughterhouse wastewater. *Revista Mexicana de Ingeniería Química 17*, 621-631. https://doi.org/10.24275/10.24275/uam/izt/dcbi/revmexingquim/2018v17n2/

Hernández-Fydrych, V.C., Benítez-Olivares, G., Meraz-Rodríguez, M.A., Salazar-Peláez, M.L., Fajardo-Ortiz, M.C. (2019). Biomass and Bioenergy Methane production kinetics of pretreated slaughterhouse wastewater. *Biomass and Bioenergy 130,* 105385. https://doi.org/10.1016/j.biombioe.2019.105385

Izumi, K., Okishio, Y. ki, Nagao, N., Niwa, C., Yamamoto, S., Toda, T. (2010). Effects of particle size on anaerobic digestion of food waste. *International Biodeterioration & Biodegradation 64*, 601-608. https://doi.org/10.1016/j.ibiod.2010.06.013

Jain, Siddharth, Jain, Shivani, Wolf, I.T., Lee, J., Tong, Y.W. (2015). A comprehensive review on operating parameters and different pretreatment methodologies for anaerobic digestion of municipal solid waste. *Renewable & Sustainable Energy Reviews 52*, 142-154. https://doi.org/10.1016/j.rser.2015.07.091

Kafle, G.K., Chen, L. (2016). Comparison on batch anaerobic digestion of five different livestock manures and prediction of biochemical methane potential (BMP) using different statistical models. *Waste Management 48*, 492-502. https://doi.org/10.1016/j.wasman.2015.10.021

Khalid, A., Arshad, M., Anjum, M., Mahmood, T., Dawson, L. (2011). The anaerobic digestion of solid organic waste. *Waste Management 31*, 1737-1744. https://doi.org/10.1016/j.wasman.2011.03.021

Kong, J., Yu, S. (2007). Fourier transform infrared spectroscopic analysis of protein secondary structures. *Acta Biochimica et Biophysica Sinica 39*, 549-559. https://doi.org/10.1111/j.1745-7270.2007.00320.x

Kong, X., Yu, S., Xu, S., Fang, W., Liu, J., Li, H. (2018). Effect of Fe 0 addition on volatile fatty acids evolution on anaerobic digestion at high organic loading rates. *Waste Management 71*, 719-727. https://doi.org/10.1016/j.wasman.2017.03.019

Labatut, R.A., Angenent, L.T., Scott, N.R. (2011). Biochemical methane potential and biodegradability of complex organic substrates. *Bioresource Technology 102*, 2255-2264. https://doi.org/10.1016/J.BIORTECH.2010.10.035

Lowry, O.H., Rosebrough, N.J., Farr, A.L., Randall, R.J. (1951). Protein measurement with the Folin phenol reagent. *Journal of Biological Chemistry 193*, 265-75.

Palatsi, J., Viñas, M., Guivernau, M., Fernandez, B., Flotats, X. (2011). Anaerobic digestion of slaughterhouse waste: Main process limitations and microbial community interactions. *Bioresource Technology 102*, 2219-2227. https://doi.org/10.1016/j.biortech.2010.09.121

Rodríguez-Abalde, Á., Gómez, X., Blanco, D., Cuetos, M.J., Fernández, B., Flotats, X. (2013). Study of thermal pre-treatment on anaerobic digestion of slaughterhouse waste by TGA-MS and FTIR spectroscopy. *Waste Management & Research 31*, 1195-1202. https://doi.org/10.1177/0734242X13507312

Shi, X., Lin, J., Zuo, J., Li, P., Li, X., Guo, X. (2016). Effects of free ammonia on volatile fatty acid accumulation and process performance in the anaerobic digestion of two typical bio-wastes. *Journal of Environmental Science 1-9*. https://doi.org/10.1016/j.jes.2016.07.006

Song, M., Shin, S.G., Hwang, S. (2010). Bioresource Technology Methanogenic population dynamics assessed by real-time quantitative PCR in sludge granule in upflow anaerobic sludge blanket treating swine wastewater. *Bioresource Technology 101*, S23-S28. https://doi.org/10.1016/j.biortech.2009.03.054

Vavilin, V.A., Fernandez, B., Palatsi, J., Flotats, X. (2008). Hydrolysis kinetics in anaerobic degradation of particulate organic material: An overview. *Waste Management 28*, 939-951. https://doi.org/10.1016/j.wasman.2007.03.028

Wang, B., Strömberg, S., Li, C., Nges, I.A., Nistor, M., Deng, L., Liu, J. (2015). Effects of substrate concentration on methane potential and degradation kinetics in batch anaerobic digestion. *Bioresource Technology 194*, 240-246. https://doi.org/10.1016/j.biortech.2015.07.034

Ware, A., Power, N. (2017). Modelling methane production kinetics of complex poultry slaughterhouse wastes using sigmoidal growth functions. *Renewable Energy 104*, 50-59. https://doi.org/10.1016/j.renene.2016.11.045

Ware, A., Power, N. (2016a). What is the effect of mandatory pasteurisation on the biogas transformation of solid slaughterhouse wastes? *Waste Management 48*, 503-512. https://doi.org/10.1016/j.wasman.2015.10.013

Ware, A., Power, N. (2016b). Biogas from cattle slaughterhouse waste: Energy recovery towards an energy self-sufficient industry in Ireland. *Renewable Energy 97*, 541-549. https://doi.org/10.1016/j.renene.2016.05.068

Yang, D., Deng, L., Zheng, D., Liu, G., Yang, H., Wang, L. (2015). Separation of swine wastewater into solid fraction, concentrated slurry and dilute liquid and its influence on biogas production. *Fuel 144*, 237-243. https://doi.org/10.1016/j.fuel.2014.12.044

Zhang, C., Su, H., Baeyens, J., Tan, T. (2014). Reviewing the anaerobic digestion of food waste for biogas production. *Renewable Sustainable Energy Reviews 38*, 383-392. https://doi.org/10.1016/j.rser.2014.05.038

Zheng, Z., Cai, Y., Zhang, Y., Zhao, Y., Gao, Y., Cui, Z., Hu, Y., Wang, X. (2021). The effects of C/N (10-25) on the relationship of substrates, metabolites, and microorganisms in "inhibited steady-state" of anaerobic digestion. *Water Research 188*, 116466. https://doi.org/10.1016/j.watres.2020.116466

Zwietering, M.H., Jongenburger, I., Rombouts, F.M., van't Riet, K. (1990). Modeling of the bacterial growth curve. *Applied Environmental Microbiology 56*, 1875-81.